Polymer(Korea), Vol. 36, No. 6, pp. 745-755
http://dx.doi.org/10.7317/pk.2012.36.6.745

ISSN 0379-153X(Print)
ISSN 2234-8077(Online)

이산화티탄 나노입자 필러가 PET와 PLA 나노복합체의 특성에 미치는 영향

Mehdi Farhoodi, Saeed Dadashi, Seyed Mohammad Ali Mousavi†, Rahmat Sotudeh-Gharebagh*, Zahra Emam-Djomeh, Abdolrasul Oromiehie**, and Farkhondeh Hemmati***

Department of Food Science & Technology, Faculty of Agricultural Engineering, University of Tehran
*School of Chemical Engineering, College of Engineering, University of Tehran
**Iran Polymer Institute
***Polymer Engineering and Color Technology Department, Amirkabir University of Technology

(2012년 5월 30일 접수, 2012년 8월 14일 수정, 2012년 8월 16일 채택)

Influence of TiO_2 Nanoparticle Filler on the Properties of PET and PLA Nanocomposites

Mehdi Farhoodi, Saeed Dadashi, Seyed Mohammad Ali Mousavi†, Rahmat Sotudeh-Gharebagh*, Zahra Emam-Djomeh, Abdolrasul Oromiehie, and Farkhondeh Hemmati*****

Department of Food Science & Technology, Faculty of Agricultural Engineering, University of Tehran, P.O.Box 31587-77871, Karaj, Iran
**School of Chemical Engineering, College of Engineering, University of Tehran, P.O. Box 11155/4563, Tehran, Iran*
***Iran Polymer Institute, Pazhuhesh Blvd. Peykanshahr, Tehran 2, Iran*
****Polymer Engineering and Color Technology Department, Amirkabir University of Technology, No. 424, Hafez ave., Tehran, Iran*

(Received May 30, 2012; Revised August 14, 2012; Accepted August 16, 2012)

Abstract: Two types of polymers were tested in this study; poly(ethylene terephthalate) (PET) as a synthetic example and poly(lactic acid) (PLA) as a natural polymer. DSC analyses showed that the use of nanofiller increased the degree of crystallinity (X_c) of both PET and PLA polymers, but the effect was more noticeable on PET nanocomposites. The crystallization of PLA and PET nanocomposites occurred at higher temperatures in comparison to neat polymers. According to dynamic mechanical-thermal analysis (DMTA), the damping factor of PET/TiO_2 nanoparticles decreased compared to the neat matrix, but for PLA nanocomposites the opposite trend was observed. Results of the mechanical test showed that for both PET and PLA nanocomposites, the most successful toughening effect was observed at 3 wt% loading of TiO_2 nanoparticles. SEM micrographs revealed uniform distribution of TiO_2 nanoparticles at 1 and 3 wt% loading levels. The results of WAXD spectra explained that the polymorphs of PLA and PET was not affected by TiO_2 nanoparticles. UV-visible spectra showed that TiO_2 nanocomposite films had high ultraviolet shielding compared to neat polymer, but there was significant reduction in transparency.

Keywords: nanocomposites, poly(lactic acid), poly(ethylene terephthalate), crystallization, mechanical properties.

Introduction

Poly(ethylene terephthalate) (PET), produced from ethylene glycol and either terephthalic acid or dimethyl terephthalate, is commonly used as a packaging material for drinking water, mineral water, carbonated beverages and edible oils. The strength and permeability properties of PET; its resistance to chemicals and its high degree of transparency are the main factors that make it superior to most other synthetic polymers. However, the use of synthetic polymers is gradually being replaced by biodegradable materials. Polymers from renewable sources have attracted increasing attention over the last two decades, for two major reasons: firstly, environmental concerns, and secondly the realization that our petroleum resources are finite.[1] Generally, polymers from renewable sources can be classified into three groups: (1) natural polymers such as starch, protein, and cellulose, (2) synthetic polymers from bio-derived monomers such as poly(lactic acid) (PLA); and (3) polymers from microbial fermentation such as

†To whom correspondence should be addressed.
E-mail: mousavi@ut.ac.ir

polyhydroxybutyrate.[2] In recent years, PLA has become increasingly popular as a biodegradable engineering plastic because of its mechanical strength and simple processing compared to other biopolymers.[3] The main limitations of this biodegradable polymer on further industrial application are its poor thermal and mechanical resistance and limited gas barrier properties compared to equivalent petroleum based polymers. These drawbacks limit its access to some industrial sectors, such as packaging, in which its use would be justified when biodegradability is required.[4] Despite abundant use of synthetic and natural polymers, in the past decades polymers reinforced with micrometer fillers have been used to obtain higher strength and stiffness; to improve solvency or fire resistance, or simply to reduce cost. However, the incorporation of these micro sized fillers has some drawbacks such as brittleness and opacity. Nanocomposites, of which at least one dimension of the filler is in the nanometer range, present an alternative approach to overcome the limitations of traditional fillers.[5] Besides, the mentioned properties, improvements in nanocomposites can be achieved at a very low loading of the nanoscale inorganic component (<5 wt%), but traditional microcomposites usually require much higher loadings (25-40 wt%).[6] However, to achieve the mentioned positive effects of nanoparticles on properties, adequate dispersion of nanofillers within the polymeric matrix is required. However, different parameters like polymer type and morphology, type and size of nanofillers, the interaction of nanofillers with the polymeric matrix and its volume content could influence the characteristics of nanocomposites. Among many different types of nano sized fillers, TiO_2 nano powder is increasingly being investigated because it is non-toxic, chemically inert, has broadband UV filter properties, is anti bacterial from its photo-irradiation effect, corrosion resistant and has high level hardness, high refractive index and low cost.[7] The effects of nano sized TiO_2 on crystallization and the viscoelastic behaviour of synthetic[8-10] and natural[11-13] polymers have been discussed in some other research. Depending on the polymeric matrix type, the addition of TiO_2 nanoparticles could increase[8] or decrease[12,13] the degree of crystallinity of nanocomposites. Other parameters like melting point, glass transition, and crystallization rate could also change according to polymer structure.[14] The purpose of this study was to investigate the role of polymer type (synthetic or natural) on physical and thermo-mechanical properties of the prepared polymer/TiO_2 nanocomposites. The effects of various levels of nanofiller loading and its dispersion were also investigated.

Experimental

Materials. Pure poly(ethylene terephthalate) (PET) (blow molding grade) with intrinsic viscosity of 0.82 dL/g was provided by Tondgooyan Petrochemical Company (Iran). Poly(lactic acid) (PLA) was purchased from Kunststoff GmbH Siemensring 79 (Germany). Anatase TiO_2 nanoparticles were supplied by Nanoshel LLC (USA). The average diameter of the particles (as recorded by the company) was about 20 nm. Chloroform solution (analytical-grade) was purchased from AppliChem (Darmstadt, Germany).

Preparation of Nanocomposites. PLA nanocomposite films were prepared by solution casting. PLA pellets were dried in a vacuum oven at 60 ºC for 24 h before nanocomposite preparation. 3 and 5 wt% solutions of PLA in chloroform were prepared by stirring the components on a plate at 50 ºC until the pellets were fully dissolved (8 h). Nanocomposites containing 3 and 5 wt% nanoparticles (coded as PLA3 and PLA5 in the following text) were prepared by adding nano TiO_2 to chloroform solutions with about 95 wt% of PLA pellets dissolved in them. The solutions were then stirred and sonified for 30 min prior to casting. The materials were then cast in Petri dishes greased with silicon and left at room temperature for a week allow the chloroform to evaporate. The prepared films had a thickness of 80 microns. Pure PLA film (coded as PLA0) was prepared in the same way. PET nanocomposites containing 3 and 5 wt% of TiO_2 (coded as PET3 and PET5 in the following parts) were prepared via melt blending in a lab-scale counter-rotating twin-screw extruder (Collin ESC-T10 model) with screw diameter of 50 mm and L/D ratio of 15. The extruder has 5 heater zones and a die zone, set at 250, 270, 275, 270, 265, and 265 ºC and operated at a screw speed of 90 rpm. Nanocomposite components were dried in an oven at 170 ºC for 5 h before the extrusion process. The prepared profiles were water-cooled and then milled using conventional milling equipment. Neat PET sample (coded as PET0) as reference material was prepared in the same procedure.

DSC Analysis. The melting and crystallization characteristics of PET and PLA in the prepared samples were studied by a differential scanning calorimeter (DSC 200 F3 Maia® NETZSCH, Germany). The melting behaviour of nanocomposite samples was determined using heating and cooling tests between 25-270 ºC for PET and 25-200 ºC for PLA at a rate of ±10 ºC/min. The first heating run used to erase the thermal history and all data were obtained from the second heating curve of the DSC thermograms. The degree of crystallinity (X_c) of

polymer in the nanocomposites and neat polymer specimens were calculated using equation (1):

$$X_c = \left(\frac{\Delta H_m}{\Delta H_{m0}}\right) \times 100 \quad (1)$$

Where ΔH_{m0} is the melting enthalpy of 100% crystalline PET and PLA ($\Delta H_{m0} = 105.97$ J/g[8] for PET and 87 J/g[15] for PLA), ΔH_m is the melting enthalpy of the samples.

Dynamic Mechanical Thermal Analysis (DMTA). DMTA experiments were carried out using single cantilever bending of PET specimens (around 30×10×2 mm^3 in size) (Polymer Laboratories, Loughborough, UK) at a frequency of 1 Hz and temperature range of 25 to 270 °C, at a heating rate of 5 °C/min. The PLA specimens (dimensions 25×5×0.08 mm^3) were tested with a tension method at a frequency of 1 Hz and at a temperature range of 25 to 90 °C, at a heating rate of 2 °C/min.

X-ray Diffraction (XRD). The XRD patterns were recorded in an X-ray diffractometer (Simens D5000-Germany) at room temperature, using CuKα tube radiation with the wavelength of 1.5409 Å, generated at 30 kV and 30 mA. The samples were scanned in the range of $2\theta = 2$–80^o with a step size of 0.04^o.

Scanning Electron Microscopy (SEM). The bulk morphology of the prepared samples was investigated using field emission scanning electron microscopy (FE-SEM; Hitachi S-4160) under an acceleration voltage of 15 kV. The specimens were fractured in liquid nitrogen and the cross surface of samples were coated by gold using a sputtering process.

Tensile Testing. Engineering stress-strain curves were prepared from uniaxial tension tests (following ASTM D638) on injection molded dumbbell-like specimens using a Galdabini Sun2500 tensile tester (Galdabini, Italy). The tensile tests were carried out at crosshead speed of 5 mm/min for PET samples and 50 mm/min for PLA samples. At least five specimens for each sample were tested. The mechanical characteristics of each sample were determined in terms of stress at break, strain at break, elastic modulus and dissipated energy.

UV-Visible Test. UV-visible spectra were recorded on Analytik-Jena Specord 250 PLUS spectrophotometer.

Three samples cut from every prepared film were used to perform tests.

Results and Discussion

Morphological Observations. SEM micrographs of PET nanocomposites showed that uniform distribution and good dispersion of TiO_2 through PET matrix were achieved at 1 and

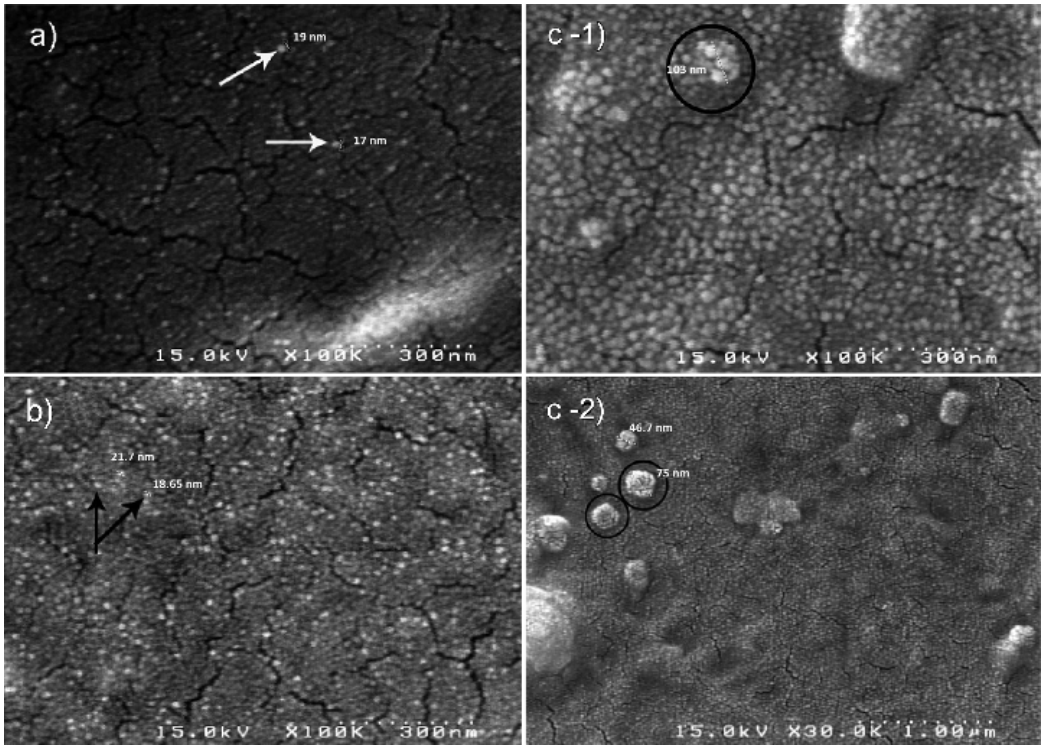

Figure 1. SEM micrographs of fracture surfaces of PET-TiO_2 nanocomposites: PET1 (a); PET3 (b); PET5 (c)-1 and (c)-2; (c)-2 is a lower magnification of PET5.

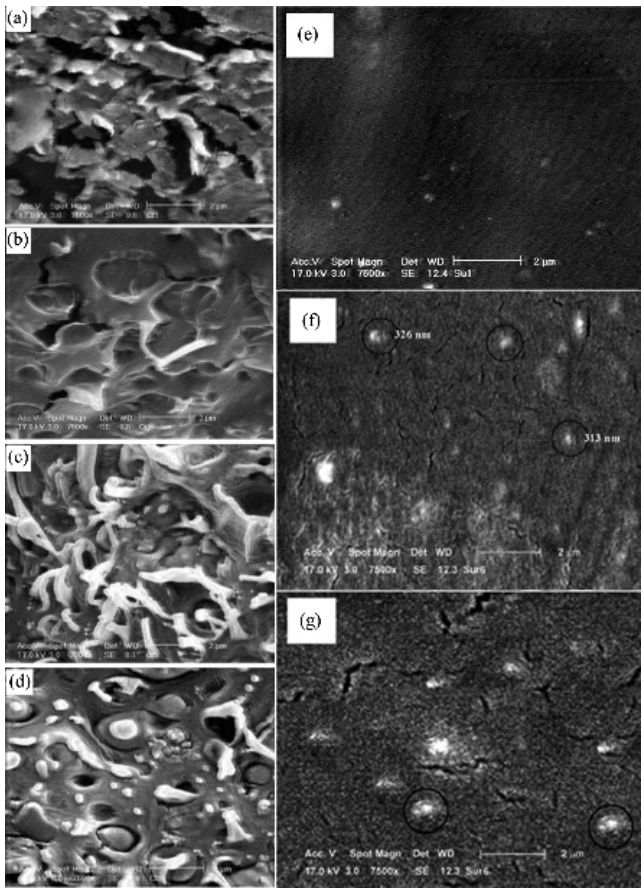

Figure 2. SEM micrographs of fracture surfaces and surfaces of neat PLA and PLA-TiO_2 nanocomposites: neat PLA (a); PLA1 (b, e); PLA3 (c, f); PLA5 (d, g).

3 wt%, while at higher loading levels of up to 5 wt%, nanoparticles tended to accumulate (Figure 1). The average size of a single TiO_2 nanoparticle is 20 nm (as mentioned in data sheet of company), however when these nanoparticles agglomerate their size can reach up to to 100 nm (Figure 1(c)-1).

According to Figure 2(e), the distribution of TiO_2 nanoparticles in PLA1 seems to be uniform with less small sized agglomerates. When the TiO_2 loading level raised to 3 wt% there was more of the larger sized agglomerates (more than 300 nm) observed in the polymer matrix (Figure 2(f)). Subsequently at higher loading levels of TiO_2 (up to 5 wt%) nanoparticles tendency to agglomerate intensified and more of the larger sized agglomeration is observed (Figrue 2(g)). This tendency is stronger for PLA nanocomposites in which agglomeration occurs at lower TiO_2 loading. Such agglomeration significantly influences the properties of nanocomposites.

Differential Scanning Calorimetry (DSC). Values for glass transition temperature (T_g), melting temperature (T_m), crystallization temperature (T_c), enthalpy of melting (ΔH_m), and the degree of crystallinity (X_c) are listed in Table 1. T_g of a polymer system varies for a variety of reasons, including changes in tacticity, molecular weight, crosslinking density, free volume, and amount of reaction residue acting as a plasticizer.[16] Table 1 shows that the reduction of T_g for PET nanocomposites with increasing TiO_2 content is not very significant. Todorov *et al.* (2009) observed an unnoticeable effect of TiO_2 nanoparticles on the glass transition point of PET.[9] However, in this study, the addition of TiO_2 nanoparticles to the PLA matrix caused a more noticeable reduction of glass transition of PLA, as the glass transition of PLA nanocomposites containing 1, 3 and 5 wt% nanoparticles decreased by 2.3, 10.1 and 9.8% compared to neat PLA, respectively. Similar results were also found in other researches by Nakayama *et al.* (2007) and Zhang *et al.* (2009).[13,17] The incorporation of nanoparticles could disturb the packing and regularity of polymer chains and cause free volume increment in a system. This effect could be more significant at higher nanoparticle contents, when more agglomerations form in the matrix. Therefore, the falling level of glass transition in PLA nanocomposites is more noticeable, which could be from the result of a higher amount of TiO_2

Table 1. Characteristic Values of DSC Analysis of Different Samples

Sample	T_g (°C)	T_m (°C)	T_c (°C)	ΔT_m (°C)	ΔH_m (J/g)	X_c (%)
PET0	81.5	249.2	187.5	20.1	35.48	33.48
PET1	80.3	250.0	191.8	22.2	35.02	33.04
PET3	80.7	249.9	193.2	30.1	42.05	39.68
PET5	80.8	250.0	191.8	21.1	34.30	32.36
PLA0	53.83	153.95	84.83	30.14	11.99	13.78
PLA1	52.59	152.19	85.61	30.02	14.01	16.10
PLA3	48.40	153.14	85.47	30.43	12.40	14.94
PLA5	48.54	152.31	86.60	29.87	11.33	12.92

agglomerate or non-uniform dispersion of nanoparticles.

Compared to neat PET, the crystallization temperatures (T_c) of PET nanocomposites shift to higher temperatures. Yamada *et al*. (2006) observed that the PET/TiO_2 nanocomposites containing 0.5, 1 and 2 wt% TiO_2 had higher crystallization temperatures compared to neat polymer.[8] In another research, it was determined that PET/$BaSO_4$ composites exhibited a higher temperature crystallization point (T_c = 203 °C) than neat PET (T_c = 191 °C).[18] The same trend was observed for PET/SiO_2 composites.[19] These observations could be due to the heterogeneous nucleation effect of nanoparticles' surface on the crystallization of PET macromolecules, which reduces the need for meeting the barrier activation energy of thermal homogeneous nucleation.[20] Therefore, the crystallization process of nanocomposites can begin at higher temperatures than pure polymer. As a result of this phenomena, the nucleation rate and consequently overall crystallization kinetics is promoted. The aforementioned reduction in the crystallization peak width could verify the increment of overall crystallization rate of the prepared nanocomposites. However, the increment in T_c values of PLA nanocomposites is not noticeable. This could be as a consequence of poor dispersion of nanoparticles in these nanocomposites. Second heating curves of pure PET and PLA and their nanocomposites are displayed in Figure 3. As shown in Figure 3, the melting points of PET nanocomposites show negligible changes comparing to the PET0 sample. However, for PLA nanocomposites, a decrease in T_m is observable especially in the case of PLA5. For PET3, the melting peak is broader (ΔT_m = 30.1 °C compared to 20.1 °C for PET0). This result is a direct consequence of broader crystallite size distribution in the presence of solid nanoparticles that could induce imperfections during the crystallite growth process. Thus, various sizes of the formed crystallites in nanocomposites with different thermal stabilities broaden the melting peaks. A comparison of the ΔT_m of different nanocomposites to that of pure polymers shows that this phenomenon could occur for nanocomposites with good dispersion and distribution of nanoparticles, while for nanocomposites with higher amounts of agglomeration the opposite action occurs (PLA3 and PLA5). Another characteristic value of the crystallization process is the final degree of crystallinity, shown in Table 1 for different prepared samples. Compared to neat PET, the sample containing 3 wt% TiO_2 has the highest X_c. As demonstrated, X_c of the prepared nanocomposites shows an optimum value with an increasing nanoparticle loading. However, when the content of TiO_2 in PET matrix increases to 5 wt%, X_c tends to decrease, suggesting high nanofiller content significantly restricts the mobility of polymer chain segments. Another important effect of the incorporation of nanofiller in to polymers and their crystallization process is that nanoparticles can create a physical hindrance to the motion of polymer chains. Thus, the nanofiller's surface and nanoparticle agglomerates could limit crystal growth, resulting in a decrease of X_c and the degree of crystallite perfection. Figure 1 shows that at lower concentrations of nanofiller (PET1 and PET3), uniform distribution and appropriate dispersion of TiO_2 nanoparticles through matrix was obtained. While, increasing the TiO_2 loading up to 5 wt% leads to nanoparticle agglomeration. Therefore, the interaction of polymer chains with higher accessible solid surfaces and embedding of a portion of macromolecule chain length in nanofiller agglomerates could significantly hinder the segmental motion of polymer chains during crys-

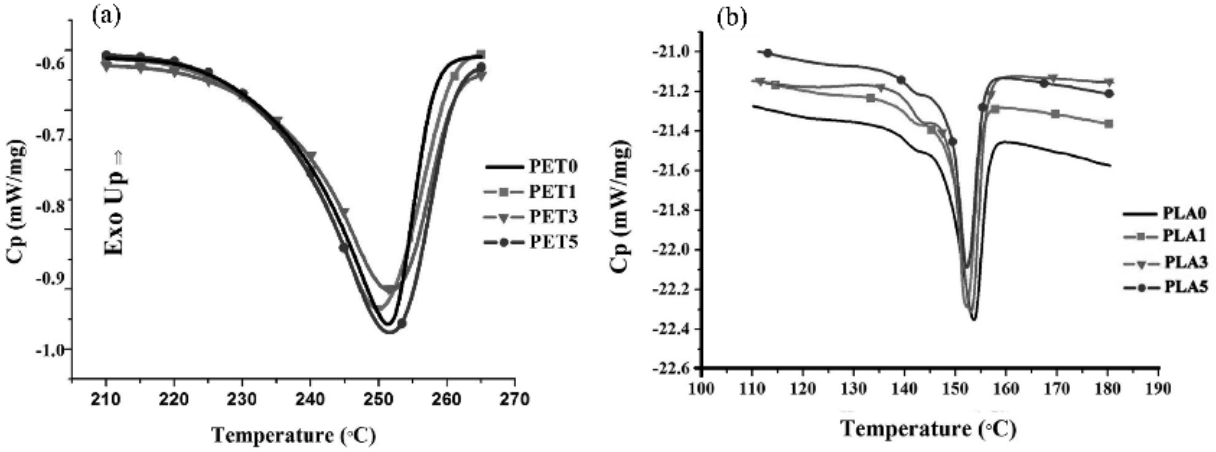

Figure 3. Second heating curves of the prepared PET (a); PLA (b) samples.

tallization. This phenomenon could be the reason that the PET5 sample showed lower X_c.

Reduction of X_c and melting point in PLA nanocomposites has been reported in other research.[17,21] Zhang, *et al*. (2009) suggested that the reason for these phenomena is probably the efficient role of TiO_2 nanoparticles in disarranging the regularity of chain structures of PLA and increasing spaces between the chains.[17] While, Liao, *et al*. (2012) stated that the lower melting temperature and crystallinity of PLA nanocomposite is due to an increment in the number of small crystallites and subsequently lower overall crystallinity of PLA in the presence of nanoparticles.[21] In this research, it seems that disarranging of PLA chains occurs at higher loading levels of TiO_2 nanoparticles as showed in Figure 2 with bigger agglomeration size (PLA3 and PLA5 as shown in Figure 2) while at 1% loading level, relatively uniform dispersion of nanoparticles results in increased crystallinity due to the nucleation effect of nanoparticles. Generally, the crystallization behaviour of nanocomposites depends on the nanofiller loading, its dispersion in the matrix and the type of matrix. Crystallization is determined by the relative dominating status of two different effects of nanoparticles on the crystallization process i.e. the nucleation effect and the growth restriction effect. At low level TiO_2 content and uniform dispersion of nanoparticles, the first effect dominates. Therefore, there is a high value X_c of PET3 and PLA1 samples. However, increasing the nanofiller loading and agglomerate formation could alter the situation in which the hindrance of macromolecule motion becomes stronger. Nucleation effects of TiO_2 nanoparticles on crystallization behaviour of PET matrix seem much stronger than on the PLA matrix.

Dynamic Mechanical Thermal Analysis (DMTA). Figures 4 and 5 represent the storage modulus (E') and tanδ of nanocomposites versus temperature, respectively.

As demonstrated in Figure 5(a), the peak position of tanδ does not change drastically for PET nanocomposites in com-

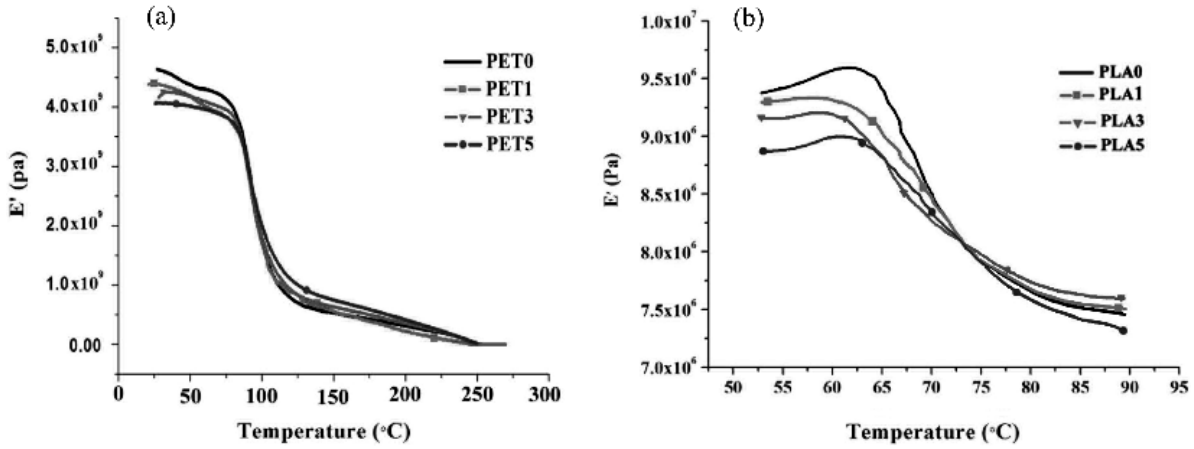

Figure 4. Storage modulus (E') of the prepared PET (a); PLA (b) samples.

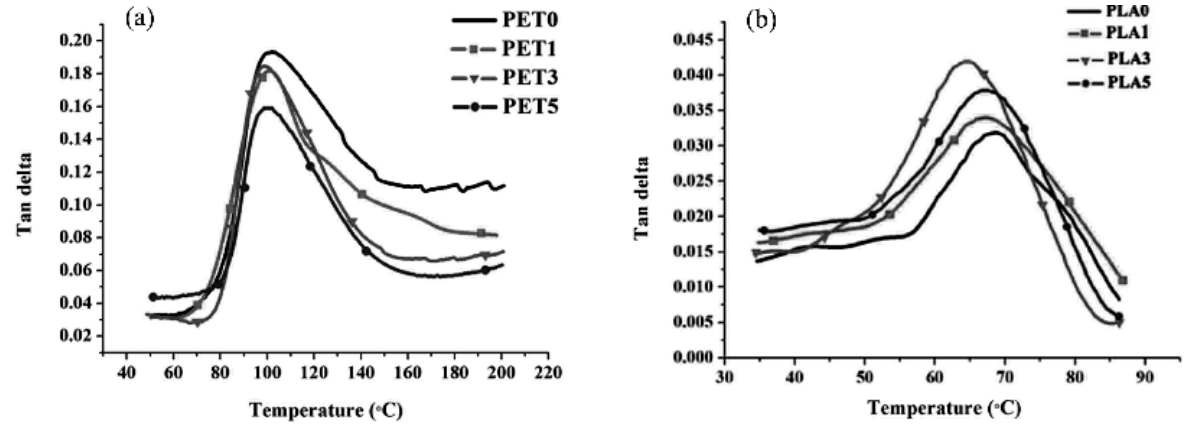

Figure 5. Tanδ of the prepared PET (a); PLA (b) samples.

Table 2. E' at 40, 80 and 140 °C and Tanδ Peak Temperature and Values for the Prepared PET and PLA Samples

Sample	E' at 55 °C (Pa)	E' at 80 °C (Pa)	E' at 140 °C (Pa)	Temp. of tanδ at peak (°C)	Tanδ peak value
PET0	4.31×10^9	3.98×10^9	0.57×10^9	101.10	0.193
PET1	4.09×10^9	3.70×10^9	0.63×10^9	101.06	0.182
PET3	4.15×10^9	3.85×10^9	0.69×10^9	98.63	0.180
PET5	3.99×10^9	3.74×10^9	0.82×10^9	99.85	0.160
PLA0	9.42×10^6	7.67×10^6	–	68.66	0.032
PLA1	9.31×10^6	7.69×10^6	–	66.94	0.034
PLA3	9.15×10^6	7.74×10^6	–	64.50	0.042
PLA5	8.88×10^6	7.58×10^6	–	66.89	0.038

E' values defined below and above the T_g values (temp. of tanδ at peak).

parison to the PET0 sample (demonstrating insignificant changes in T_g values verifying DSC results), while magnitudes of the tanδ peak decrease with an increased TiO_2 loading. It could verify that these prepared nanocomposites have lower damping capability than pure PET. This reduction is more noticeable for nanocomposites containing 5 wt% nanofiller. It was found that with an addition of inorganic filler such as carbon black, silica and metal oxide/hydroxide to a polymer matrix leads there is a decrease in the tanδ value.[22] This reduction can be a consequence of the polymer chain interaction with the solid surface of fillers that restricts polymer segmental motion and lowers the damping capability of the material. The natural polymer used in this study showed the opposite activity. Figure 5(b) shows that PLA nanocomposites demonstrate higher damping capability than neat PLA.

Additions of 3 wt% TiO_2 nanoparticles into the PLA resulted in maximum damping capability, but with an addition of TiO_2 nanoparticles up to 5 wt%, the tanδ value tends to decrease. As demonstrated by the results for DSC, an addition of nanoparticles to the PLA matrix disarranges the regularity of polymer chains and increases the total free volume of the nanocomposite. As a result, the damping capability or the tanδ value at peak of nanocomposite is promoted. The temperature taken to reach the tanδ peak (defined as T_g) inclines to a lower temperature with incorporation of TiO_2 nanoparticles in the PLA structure. These results are absolutely adopted with T_g value variation trends of nanocomposites obtained by DSC. As listed in Table 2, the minimum T_g value conforms to the maximum tanδ peak value for PLA3 nanocomposite that explains the maximum damping effect of nano-TiO_2.

Table 2 shows that the storage modulus of PET samples varies between 3.99 to 4.31 GPa at 55 °C; 3.74 to 3.98 GPa at 80 °C and 0.57 to 0.82 GPa at 140 °C depending on the level of nanofiller loading from 0 to 5 wt%. The increase of storage modulus above the T_g point could be as a result of the formation of a network structure between TiO_2 particles via polymer chains that increases the rigidity of the nanocomposites. This trend has been reported by other authors[23,24] and it supports the decreasing effect of tanδ of nanocomposites, which reaches the lowest value in a nanocomposite containing 5 wt% TiO_2. The storage modulus of PLA nanocomposites varies between 8.88 to 9.42 MPa at 55 °C and 7.58 to 7.74 MPa at 80 °C depending on the level of nanofiller loading from 0 to 5 wt%. Below the glass transition point the storage modulus of PLA nanocomposites decreases with incremental TiO_2 loading but for temperatures above that of the level for glass transition, the storage modulus first increase with additions of 1 and 3 wt% TiO_2 and subsequently decreases with a higher level loading of nanoparticles. As mentioned in the previous section, for PLA5 sample a higher amount of nanoparticle agglomerates formed. These agglomerates could disturb the formation of the aforementioned physical network that is responsible for reinforcing the polymer matrix and increasing the storage modulus above T_g.

Tensile Testing. The mechanical properties of neat polymers and prepared nanocomposites were listed in Table 3. It was expected that the elastic modulus of nanocomposites would increase with the addition of mineral rigid nanoparticles, but results collected in Table 3 show that there is not a significant difference in the magnitude of modulus of nanocomposites from that of pure polymers. Large standard deviation of the modulus values causes an overlap in the results of different samples.

As demonstrated, the tensile strength of nanocomposites

Table 3. Mechanical Properties of Neat PET, Neat PLA and Their Nanocomposites

Sample	Stress at break(MPa)	Strain at break(%)	Elastic modulus(MPa)	Dissipated energy(J)
PET0	59.6 ± 2.9	5.2 ±1.6	2467.2 ± 198.5	3.8 ± 0.6
PET1	28.3 ± 6.5	21.5 ± 4.5	2486.1 ± 96.5	4.7 ± 1.7
PET3	30.7 ± 2.0	28.3 ± 3.4	2561.3 ± 191.7	9.4 ± 2.3
PET5	36.9 ± 5.8	15.3 ± 2.6	2572.8 ± 103.2	7.1 ± 1.3
PLA0	27.44 ± 2.75	24.53 ± 1.60	1840 ± 110	3.78 ± 0.21
PLA1	26.33 ± 3.54	29.86 ± 2.33	1710 ± 140	3.85 ± 0.24
PLA3	25.14 ± 4.23	38.50 ± 3.42	1780 ± 150	5.25 ± 0.35
PLA5	23.47 ± 2.54	35.82 ± 2.64	1660 ± 170	4.42 ± 0.28

decreased compared with that of neat polymer. This could be attributed to the preventative effect of nanoparticles on strain hardening of the polymer chains after cold drawing. This strain hardening phenomenon plays a critical role in stabilizing polymers against strain localization, fracture and reducing wear.[25] So, it can be determined that nanofiller, as heterogeneous solid nanoparticles, could hinder polymer stress induced crystallization and subsequently decrease resistance of the polymer network against fracture. Another attractive effect of the addition of nanoparticles on mechanical properties is the increment of strain at break and dissipated energy or ductility (lost energy determined from the area under the stress-strain curve up to break). In the other words, the nanocomposite ductility enhanced with an addition of TiO_2 nanofiller. Incorporation of TiO_2 nanoparticles in to the PET matrix increased the strain at break of PET1, PET3 and PET5 nanocomposites by 313, 444 and 192%, respectively. Also the strain at break of PLA1, PLA3 and PLA5 nanocomposites comparing to neat PLA increased by 22, 57 and 46%, respectively. This effect could be as a consequence of the creation of new energy damping mechanisms in the presence of nanoparticles such as the breaking up of agglomerates, void nucleation, crack deflection, nanofiller debonding or pull out, matrix deformation and bridging. During occurrence of the first two mechanisms, particle agglomerates are broken up and debonded from the matrix, creating smaller or larger voids. The breaking up or debonding stress determines the crazing stress, which is lower than that in an unfilled matrix. Therefore, slight agglomeration facilitates crazing and more crazes can be created with a positive effect on energy dissipation and toughness.[26] However, as observed in Table 3, the levels of dissipated energy of PET5 and PLA5 decreased compared to those of PET3 and PLA3 samples, respectively. As the nanoparticle size increases and large agglomerates are formed, the total particle/matrix interfacial surface area available for energy dissipation decreases, but the critical stress for particle/matrix debonding also decreases and this could be the reason for observation of an optimum level of ductility with increasing nanoparticle loading. In similar research, it was found that incorporation of TiO_2 to PET could cause an increase of elongation at break.[9] The maximum toughening effect of nanoparticles in the PLA3 sample shows the highest amount of dissipated energy in tensile tests, confirmed by DMTA results. The micrographs obtained by SEM also verify these results (Figure 2(a)-(d)). At 3 wt% loading of TiO_2 in PLA, the crazes at sample surface reach its minimum level and an increased toughening effect is observed on the fracture surface (Figure 2(c)). Energy dissipation and reinforcement mechanisms work well only if a special state of particle dispersion is reached. As demonstrated, in nanocomposites containing 3 wt% of TiO_2 in which more homogenous dispersion of nanoparticles is achieved, the dissipation and reinforcement mechanisms are more active. When nanoparticles have an optimum distance from each other and are uniformly dispersed in a matrix, there is a transition from brittle failure (in the neat polymer) towards tough failure behaviour (in nanocomposites).

X-ray Diffraction. To investigate the influence of TiO_2 nanoparticles on the crystalline structure, WAXD spectra of pure TiO_2, the neat polymers and the prepared nanocomposites were obtained. The results are shown in Figure 6. The incorporation of nanoparticles to pure polymers and increasing its loading causes no shift in the peak position of crystalline planes of PET and PLA verifying that the type of crystals do not alter in the presence of TiO_2. As demonstrated, by considering peak intensities, PET3 and PLA1 samples show a higher content of crystalline structure compared to pure polymers. While for nanocomposites including higher loading of nanoparticles, peak intensities reduce. These consequences confirm the results

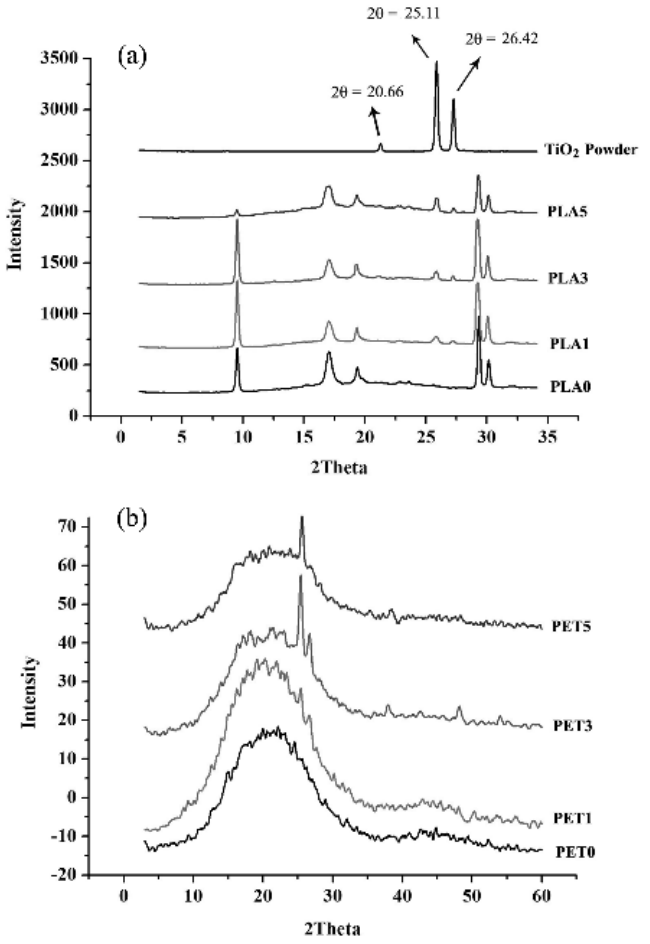

Figure 6. WAXD spectra of anatase TiO_2, neat PLA and its nanocomposites (a); neat PET and its nanocomposites (b).

of DSC analysis, in that the highest degrees of crystallinity are obtained in PET and PLA nanocomposites with 3 and 1 wt% TiO_2, respectively. At these contents, the role of nanoparticles in the creation of heterogeneous nucleation sites is dominated. The crystalline peaks of TiO_2 powder also can be observed in different nanocomposites' spectra and the intensities are related to the content of nanoparticles in these samples.

Optical Properties. Figure 7 represents UV-Vis spectra of the prepared films. Each graph establishes a comparison between the polymer film, and the fabricated nanocomposites. The influence of TiO_2 nanoparticles on optical transmission of nanocomposite films is observed both in the UV region (250-400 nm) and in the visible range (400-800 nm). From these graphs, it is evident that a considerable decrease in transmittance is observed in TiO_2 nanocomposites in comparison with neat polymer. In particular, the transmittance was null below 300 nm, in the UV region. TiO_2 nanocomposites had an effective UV-shielding property, but this lack of transparency may be due to an inherent opacifying nature of titanium dioxide. Also, inefficient nanoparticle dispersion of TiO_2 nanofillers especially at higher loading levels causes more transmission loss of PLA nanocomposite films.

Table 4 lists transmittance data values for neat PET, neat PLA and their nanocomposites. The transmittances were recorded at 370, 500, 650 and 800 nm. These nanofillers caused a considerable visible transmission loss in the films, so that the visible transmission at 500 nm wavelengths diminished from above 80% to below 20% in PET nanocomposites, and from above 20% to below 15% in PLA nanocomposite films. Espejo *et al*. (2012) observed that incorporation of 2 wt% of TiO_2, SiO_x and ZnO nanoparticles reduced the visible transmission of LDPE films from 86.5% to 32.7, 83.25 and 75.18%, respectively.[27] The maximum UV-transmission loss was also observed with TiO_2 nanoparticles compared to SiO_x and ZnO fillers. Sunay *et al*. (2012) observed that the trans-

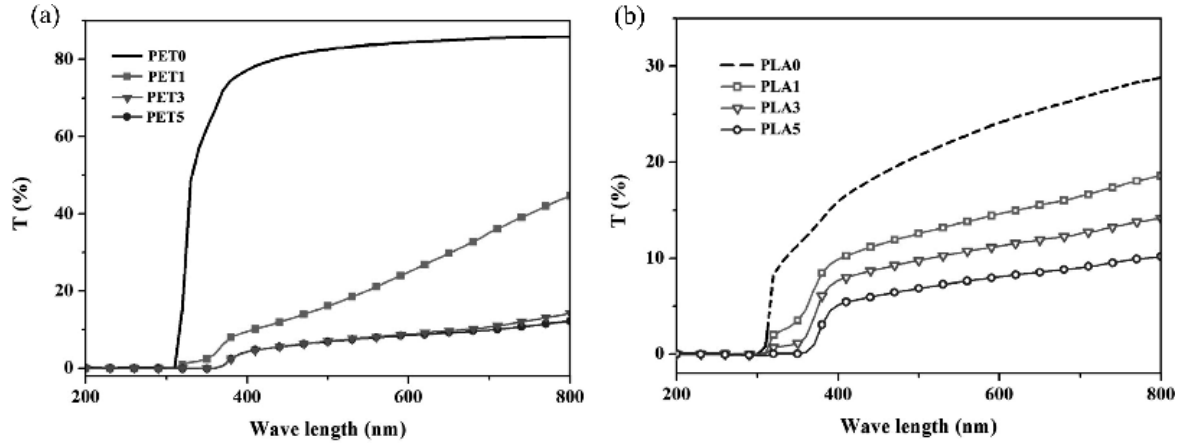

Figure 7. PET (a); PLA (b) nanocomposite films: UV-Vis spectra.

Table 4. Transmittance Data of Neat PET, Neat PLA and Their Nanocomposites

Sample	Transmittance (%)			
	370 nm	500 nm	650 nm	800 nm
PET0	72.04	82.67	84.97	85.98
PET1	6.22	16.12	29.83	44.64
PET3	0.80	7.04	9.72	14.25
PET5	0.67	6.89	9.20	12.20
PLA0	13.09	20.71	25.47	28.83
PLA1	6.71	12.56	15.52	18.60
PLA3	3.76	9.77	11.92	14.16
PLA5	0.96	6.86	8.54	10.17

parency of polystyrene film decreased when TiO_2 fillers were incorporated in to the polymer matrix.[28]

In this study, maximum transmittance was found for the neat PET sample (Table 4). Actually, the transparency of these nanocomposites depends on the nature of the polymer matrix as well as the size and distribution of nanofillers. At higher loading levels of TiO_2 particles, the tendency for agglomeration results in enhanced reduction of film transmittance.

Conclusions

Results of the DSC analysis showed that the crystallization temperatures of PET and PLA nanocomposites was higher with increasing TiO_2 loading in the polymer matrix and that the percentage of crystallinity first increases and then decreases with incremental additions of TiO_2. Degrees of crystallinity in PLA and PET nanocomposites reach maximum values in nanocomposites containing 1 and 3 wt% nanoparticles, respectively, but this effect is more evident in PET nanocomposites. These results demonstrate that an addition of TiO_2 could significantly enhance the rate of PET crystallization as a result of heterogeneous nucleation effect of TiO_2. Morphological observations show that nanoparticle dispersion is more homogenous in a PET matrix than in a PLA matrix. Dynamic mechanical analyses show that the peak position of tanδ does not change drastically for PET nanocomposites in comparison to the pure PET sample (demonstrating insignificant changes in T_g values) but in PLA nanocomposites it tends to lower temperatures. This confirms the results obtained by DSC. In PET nanocomposites the magnitudes of tanδ peak decrease according to the increased loading of TiO_2 nanoparticles while it increases in PLA nanocomposites. The results of the tensile test show that elongation at break and dissipated energy increase with additions of TiO_2 nanoparticles into PET and PLA matrices that reach the maximum amount at 3% loading level of TiO_2. These improvements of ductility could be as a result of new damping mechanisms that are more active in homogenous dispersion and distribution of nanoparticles. The XRD patterns show that incorporation of nanoparticles to the pure matrices and increasing its loading causes no shift in the peak position of crystalline planes. According to UV-Visible spectra, both PET and PLA nanocomposite films exhibited high UV shielding with transparency loss.

References

1. L. Yu, K. Dean, and L. Li, *Progr. Polym. Sci.*, **31**, 576 (2006).
2. L. Yu and L. Chen, *Polymeric materials from renewable resources. Biodegradable polymer blends and composites from renewable resources*, John Wiley & Sons Inc., pp. 1-15 (2009).
3. J. Lunt, *Polym. Degrad. Stabil.*, **59**, 145 (1998).
4. R. P. Singh, J. K. Pandey, D. Rutot, Ph. Degee, and Ph. Dubois, *Carbohyd. Res.*, **338**, 1759 (2003).
5. M. Rosoff, *Nano-surface Chemistry*, Marcel Dekker Inc., New York, 2002.
6. C. Saujanya and S. Radhakrishnan, *Polymer*, **42**, 6723 (2001).
7. D. H. Solomon and D. G. Hawthorne, *Chemistry of Pigments and Fillers*, John Wiley & Sons Inc., New York, 1983.
8. T. Yamada, L. Hao, K. Tada, S. Konagaya, and G. Li, *Mater. Sci.*, **2**, 154 (2006).
9. L. V. Todorov, C. I. Martins, and J. C. Viana, *Solid State Phenomena*, **151**, 113 (2009).
10. L. V. Todorov and J. C. Viana, *J. Appl. Polym. Sci.*, **106**, 1659 (2007).
11. L. Yonghui, Ch. Caihong, L. Jun, and S. S. Xiuzhi, *Polymer*, **52**, 2367 (2011).
12. L. Xili, L. Xiuqian, S. Zhijie, and Zh. Yufeng, *Eur. Polym. J.*, **44**, 2476 (2008).
13. N. Nakayama and T. Hayashi, *Polym. Degrad. Stabil.*, **92**, 1255 (2007).
14. J. W. Rhim, S. I. Hong, and C. S. Ha, *Tensile, LWT- Food Science and Technology*, **42**, 612 (2009).
15. E. W. Fisher, H. J. Sterzel, and G. Wegner, *Kolloid-Zeitschrift and Zeitschrift Fur Polymere*, **251**, 980 (1973).
16. Y. Y. Sun, Z. Q. Zhang, K. S. Moon, and C. P. Wong, *J. Appl. Polym. Sci.*, **42**, 3849 (2004).
17. Y. C. Zhang, J. N. Huang, H. Y. Wu, and Y. P. Qiu, *Mater. Sci.*, **613**, 316 (2009).
18. M. H. Qu, Y. Z. Wang, C. Wang, X. G. Ge, D. Y. Wang, and Q. Zhou, *Eur. Polym. J.*, **41**, 2569 (2005).
19. J. P. He, H. M. Li, X. Y. Wang, and Y. Gao, *Eur. Polym. J.*, **42**, 1128 (2006).
20. T. Wan, L. Chen, Y. C. Chua, and X. Lu, *J. Appl. Polym. Sci.*, **94**,

1381 (2004).
21. X. Liao, A. Nawaby, and H. E. Naguib, *J. Appl. Polym. Sci*., **124**, 585 (2012).
22. S. Pattanawanidchai, P. Saeoui, and C. Sirisinha, *J. Appl. Polym. Sci.*, **96**, 2218 (2005).
23. P. C. Chiang, W. T. Whang, and M. H. Tsai, *Thin Soild Films*, **447**, 359 (2004).
24. M. H. Tsai, S. J. Liu, and P. C. Chiang, *Thin Solid Films*, **515**, 1126 (2006).
25. Y. J. Mergler and R. P. Schaake, *J. Appl. Polym. Sci*., **92**, 2689 (2004).
26. L. Sun, R. F. Gibson, F. Godaninejad, and J. Suhr, *Compos. Sci. Technol.*, **69**, 2392 (2009).
27. C. Espejo, A. Arribas, F. Monzó, and P. P. Díez, *J. Plast. Film Sheet*., DOI: 10.1177/8756087912439058 (2012).
28. M. S. Sunay, O. Pekcan, and S. Ugur, *J. Nanomater.*, DOI: 10.1155/2012/524343 (2012).